Effects of confining stress and suction on volume change and shear strength behaviour of a collapsible soil

S. Almahbobi, S. Tripathy & P. J. Cleall
Geoenvironmental Research Centre, School of Engineering, Cardiff University, Cardiff, UK

ABSTRACT: Saturated and unsaturated triaxial shear strength tests were carried out on compacted specimens of a prepared soil. The composition of the soil used was similar to that found in naturally occurring aeolian soil deposits. The volume change and shear strength of the soil were determined at several matric suctions and net confining stresses during the wetting process. The relationship between suction and suction stress (i.e., suction stress characteristic curve, SSCC) was established from the wetting water retention data at various applied confining stresses and suctions. Similarly, the SSCC was established based on the shear strength test data. The results showed that the SSCCs based on the water retention behaviour and from the triaxial shear strength tests on the soil were very similar.

1 INTRODUCTION

Collapsible soils are known to withstand relatively high stresses at unsaturated state. Upon exposure to a saturation front at a constant surcharge, the volume change of such soils usually occurs within a short time period (Barden et al. 1973; Lawton et al. 1992; Pereira & Fredlund 2000). The meta-stable structure of collapsible soils is associated with the cementation provided by the fine-grained soil fractions at the inter-particle contacts of coarse fractions in the soils. With an increase in the water content or a decrease in soil suction, the cementation at the inter-particle contacts weakens. The collapse of the open pore structure in collapsible soils is due primarily to a decrease in the shear strength at interparticle level.

The effects of a decrease in matric suction on the volume change and shear strength of collapsible soils can be studied by carrying out unsaturated triaxial tests. It has been shown that the magnitudes of collapse strain and the shear strength depend upon the applied stress and suction (Fredlund et al. 2012). Since the amount of water present and the magnitude of the suction control the volume change and shear strength of unsaturated soils, studies covering the step-wise suction reduction and its impact on the volume change and shear strength are expected to provide a thorough understanding of the macroscopic behaviour of collapsible soils.

Lu and Likos (2006) stated that suction stress characteristic curve represents the stress state of the soil. Studies in the past have provided some key validations of suction stress approach based on the shear strength and volume change behaviour of soils (Baille et al. 2014; Oh & Lu 2014; Oh et al. 2013; Lu et al. 2010; Lu & Likos 2006). Oh et al. (2012) has shown that suction stress based on water retention tests and that determined from the shear strength tests remained within tens of kilopascals. These studies have provided some significant step forward to consider effective stress as the sum of net stress and suction stress.

Detailed studies of the SSCCs of collapsible soils derived from both shear strength and volumetric variables under triaxial conditions and for a large range of suction and higher stress levels are very limited. The objective of this study is to explore the impact of net confining stress and suction on the volume change and shear strength behaviour of a collapsible soil.

2 SUCTION STRESS

Lu and Likos (2006) extended Bishop's effective stress by modifying the matric suction contribution to the effective stress as follows:

$$\sigma' = (\sigma - u_a) - \sigma^s \tag{1}$$

where, σ' is the effective stress; σ is the total stress; u_a is pore air pressure; $(\sigma - u_a)$ is the net normal stress and σ^s is the suction stress.

Lu et al. (2010) established closed-form equations for suction stress, either as a function of suction (u_a –

u_w) (Equation 2) or effective degree of saturation (S_e) (Equation 3).

$$\sigma^s = -(u_a - u_w)\left[\frac{1}{1+\{\alpha(u_a - u_w)\}^n}\right]^{1-1/n} \quad (2)$$

$$\sigma^s = -\frac{S_e}{\alpha}\left[S_e^{\frac{n}{1-n}} - 1\right]^{1/n} \quad (3)$$

where, u_w is the pore water pressure and α and n are empirical fitting parameters corresponding to the air entry and pore size distribution, respectively. The effective degree of saturation (S_e) can be calculated based on the suction - degree of saturation (S_r) relationship and the residual degree of saturation (S_{res}) of the soil from Equation (4). The best-fit parameters (α and n) that are required for establishing suction stress chracteritic curves (SSCCs) in terms of suction and effective degree of saturation using Equations (2) and (3) can be determined from the suction – effective degree of saturation relationship using Equation (5).

$$S_e = \frac{S_r - S_{res}}{1 - S_{res}} \quad (4)$$

$$S_e = \left[\frac{1}{1+\{\alpha(u_a - u_w)\}^n}\right]^{1-1/n} \quad (5)$$

Lu et al. (2010) stated that if $n \leq 2$, the suction stress decreases with an increase in suction, whereas if $n > 2$, the suction stress decreases and then increases with an increase in suction. Lu et al. (2010) noted that the air-entry parameter (α) controls the minimum value of suction stress, whereas the pore size distribution parameter (n) controls the effective degree of saturation corresponding to the minimum suction stress.

The SSCC of soil can also be established from unsaturated shear strength tests. Suction stress at a known suction value can be calculated from the stress state at failure from Equation (6) (Oh et al. 2014).

$$\sigma^s = \frac{d + M(p-u_a)_f - q_f}{M} \quad (6)$$

where, p = mean stress (= (σ_1 + 2σ_3)/3) and q = deviatoric stress (= σ_1 - σ_3), σ_1 and σ_3 are the major and minor principal stresses, respectively; M is the slope of the failure envelope and d is the intercept of the failure envelope corresponding to the saturated condition. The subscript f refers to the state of failure.

3 MATERIALS AND METHODS

3.1 *Soil used*

The soil used in this investigation was a prepared soil. A mixture of M400 silt (40%), Leighton Buzzard sand (40%) and 20% Speswhite kaolin was considered for preparing the soil. These materials are available commercially from various agencies. The percentages of various particle-size fractions in the soil are similar to that found in many aeolian soil deposits, such as loess, loessic deposits and loess-derived sediments (Derbyshire & Mellors 1988). The basic properties of the soil are shown in Table 1.

Compacted soil specimens were prepared by statically compacting soil-water mixture at an initial water content of 10% and a dry unit weight of 15 KN/m^3. The diameter and height of the specimens for saturated and unsaturated triaxial tests were 50 and 100 mm, respectively.

Table 1. Properties of the soil used.

Index property	Value
Specific gravity	2.65
Atterberg limits	
Liquid limit, *LL* (%)	24
Plastic limit, *PL* (%)	16
Plasticity index, *PI* (%)	8
Shrinkage limit, *SL* (%)	10.7
Particle size distribution	
Sand (%)	40
Silt (%)	40
Clay (%)	20
BS light compaction characteristics	
Maximum dry unit weight (kN/m^3)	18.5
Optimum water content (%)	13.3
Mineralogy	
Quartz (%)	86
Kaolinite (%)	14
Unified soil classification system (USCS)	CL

3.2 *Triaxial tests*

The triaxial shear tests were conducted using two seprate GDS automated triaxial devices, such as a conventional triaxial device and an unsaturated triaxial device (HKUST-type). Consolidated drained tests were carried out on compacted-saturated specimens at confining stresses of 100, 250 and 400 kPa following guidelines laid out in BS 1377-8 (1990). The soil specimens were saturated by increasing the back pressure and cell pressure in equal increments until a *B*-value of 0.97 was achieved. The specimens were consolidated by increasing the cell pressure to the predetermined values. The rate of axial displacement during the shearing stage was 0.0015 mm/min. The tests were terminated at an axial strain of 25%.

The air-entry value of the ceramic disc used in the unsaturated triaxial device was 500 kPa.

For imposing suction in soil specimens, the pore-air pressure was applied through a coarse low air–entry disk placed on top of the soil specimens, whereas the pore-water pressure below the saturated high air–entry ceramic disk was maintained at 0 kPa. The total volume change of the specimens was measured based on the change in water level in an inner cell using a differential pressure transducer (Ng & Menzies 2007).

The unsaturated triaxial tests were carried out by step-wise wetting a soil specimen under predetermined isotropic stress followed by a consolidated drained shearing test. In total twelve identical compacted specimens were used under various magnitudes of applied matric suction, and net mean stress (Table 2). Each specimen was placed on the pedestal of the unsaturated triaxial device. The specimens were first subjected to an isotropic stress of 20 kPa. The suction of the specimens was reduced to 500 kPa at this isotropic stress. Once the applied suction of 500 kPa was equilibrated (i.e., when there was no change in total and water volumes), the isotropic stress was increased to a predetermined value from 100, 250, and 400 kPa. At each applied isotropic stress, the suction of specimens was further reduced to 300, 100, 50, and 20 kPa. A suction step was considered to be completed when a change in the rates of total and water volume were less than 0.1 cm^3/day. As can be seen in Table 2, multiple specimens were tested at each applied isotropic stress. During the shearing stage, the specimens were sheared under the drained condition by increasing the deviatoric stress at a sufficiently slow displacement rate of 0.0015 mm/min (Rampino et al. 1999). The shearing stage was terminated at an axial strain of 25% in all cases.

Table 2. Details of various stresses considered during unsaturated triaxial shear strength tests.

Sample No.	σ_3 (kPa)	u_a (kPa)	u_w (kPa)	$(\sigma_3 - u_a)$ (kPa)	$(u_a - u_w)$ (kPa)
1	400	300	0	100	300
2	200	100	0	100	100
3	150	50	0	100	50
4	120	20	0	100	20
5	550	300	0	250	300
6	350	100	0	250	100
7	300	50	0	250	50
8	270	20	0	250	20
9	700	300	0	400	300
10	500	100	0	400	100
11	450	50	0	400	50
12	420	20	0	400	20

3.3 *Initial suction and water retention behaviour of the soil at high suctions*

The initial suction of the compacted soil specimen and the water retention behaviour of the soil at high suctions were determined by using a chilled-mirror dew-point potentiameter (Leong et al. 2003). The device used was WP4C potentiameter. The initial suction of the compacted specimen corresponding to the water content of 10% and a dry unit weight of 15 kN/m^3 was found to be 563 kPa. For establishing the water retention behaviour at high suctions, specimens were prepared by static compaction method at different initial water contents and a constant dry unit weight of about 15 KN/m^3. The suctions of the compacted specimens were measured using the device. The suction – degree of saturation relationship at high suctions from chilled-mirror dew-point tests and the test results from the triaxial tests (based on the water volume and total volume changes) enabled establishing the water retention curve and suction stress characteristic curves of the soil for a large range of suction and degree of saturation.

4 RESULTS AND DISCUSSION

4.1 *Water absorption behaviour and suction stress*

Figure 1 shows the suction versus volumetric strain plot of the specimens at confining stresses of 100, 250 and 400 kPa. The specimens exhibited reductions in volume due to the applied isotropic stresses at constant suction of 500 kPa. Further, the test results showed that at any applied suction, the volumetric strain due to collapse was greater for the specimen with a higher applied isotropic stress.

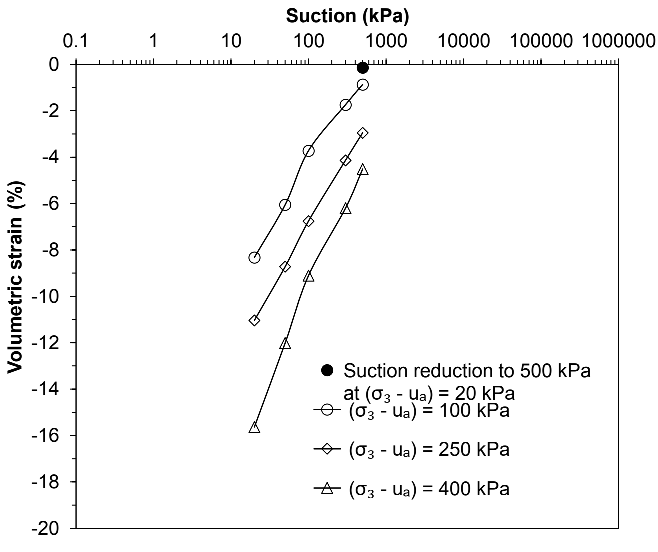

Figure 1. Variation in volumetric strain with suction at various confining stresses during the wetting process.

The test results for the water absorption of the soil specimens from unsaturated triaxial tests (prior to the shearing process) and the chilled-mirror dew-point tests are shown in Figure 2. The test results presented in Figure 2 are in terms of the effective degree of saturation. The effective degree of saturation values were calculated based on the volume change measurements and with the residual degree of saturation as 6% from Equation 4. The experimental data in Figure 2 were best-fitted with van Genuchten model (Equation 5). It can be seen from Figure 2 that the soil-water characteristic curve (SWCC) shifted slightly to the right with an increase in the confining stress.

Table 3 shows the values of α and n and the correlation coefficient (R^2) for the SWCCs at confining stresses of 100, 250 and 400 kPa. The results showed that the effects of the confining stress on α and n were not significant. In all cases, the values of n remained less than 2.0.

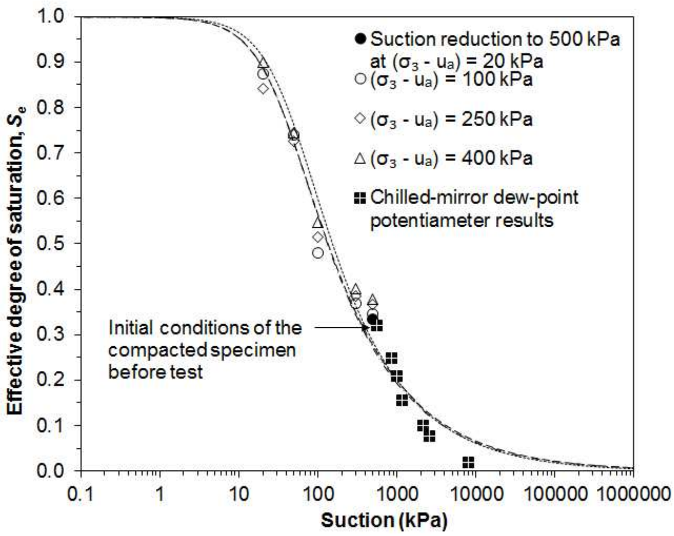

Figure 2. Suction-effective degree of saturation SWCCs at various confining stresses during the wetting process.

Table 3. SWCC model parameters at various confining stresses.

Confining stress $(\sigma_3 - u_a)$ (kPa)	Parameters		
	α (1/kPa)	n	R^2
100	0.029	1.490	0.998
250	0.029	1.479	0.997
400	0.023	1.509	0.998

The suction stress characteristic curves in terms of suction and effective degree of saturation are shown in Figures 3 and 4. These results are calculated based on Equations (2) and (3). The influence of confining stress on the SSCCs was found to be insignificant for the soil studied.

The results presented in Figure 3 show that the magnitude of suction stress is about 100 kPa at an applied suction of 500 kPa. With a decrease in suction, suction stress increased (or became less negative). At smaller applied matric suctions, the values of suction stress followed the line, - $\sigma^s = (u_a - u_w)$. The shape of the SSCCs in terms of suction was found to be in accordance with the n value (Lu et al. 2010) that were less than 2.0 for all cases.

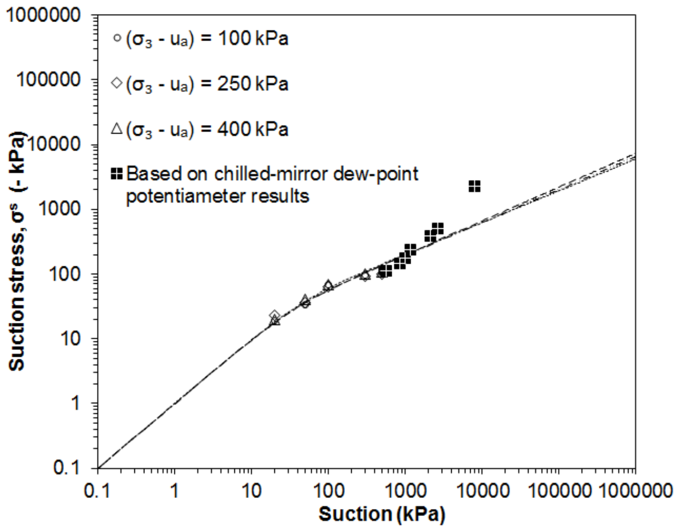

Figure 3. Suction stress characteristic curves in terms of suction at various confining stresses based on water absorption and volume change.

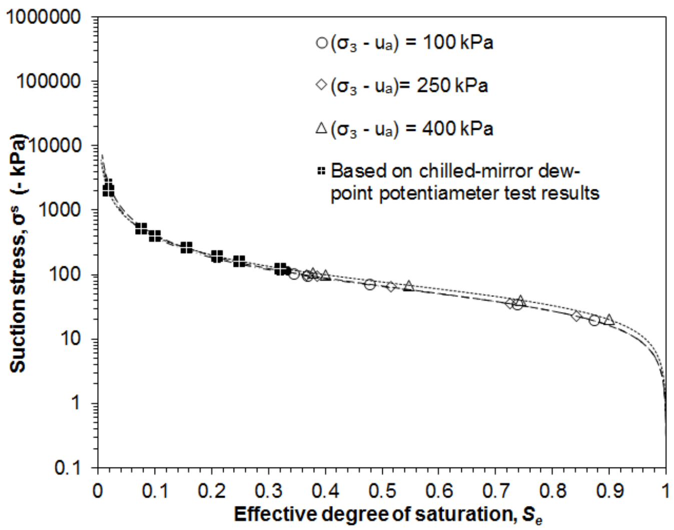

Figure 4. Suction stress characteristic curves in terms of effective degree of saturation at various confining stresses based on water absorption and volume change.

4.2 *Shear strength and suction stress*

Figure 5 shows axial strain versus deviatoric plots for the twelve specimens tested in the unsaturated triaxial device. The test results for the saturated specimens that were tested in a conventional triaxial device are also included in Figure 5. The peak shear stress increased with an increase in the confining stress and matric suction.

Figure 6 presents the Mohr circles and the failure envelopes for the saturated and unsaturated shear strength tests. The peak deviatoric stress values (Fig. 5) were considered for establishing the Mohr circles. The failure envelopes shown in Figure 6 provided the values of slope angle (ϕ') and the cohesion intercept (c) corresponding to various applied suctions. With an increase in the applied suction, the failure envelopes for unsaturated soil specimens were shifted in an upward direction.

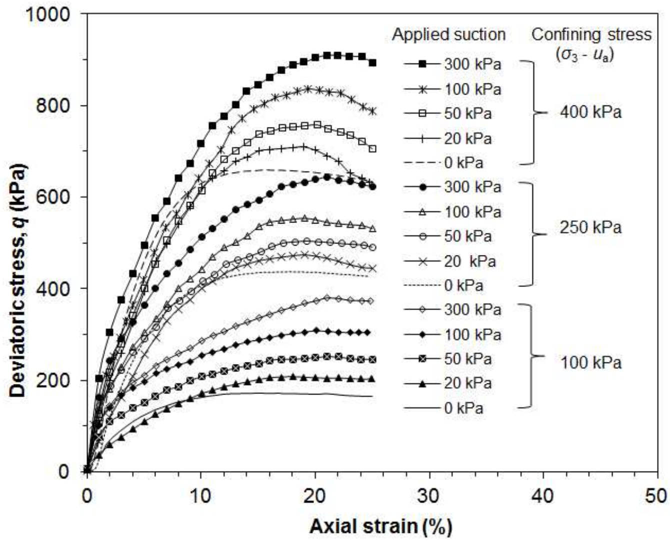

Figure 5. Axial strain versus deviator stresses plots for unsaturated and saturated soil specimens.

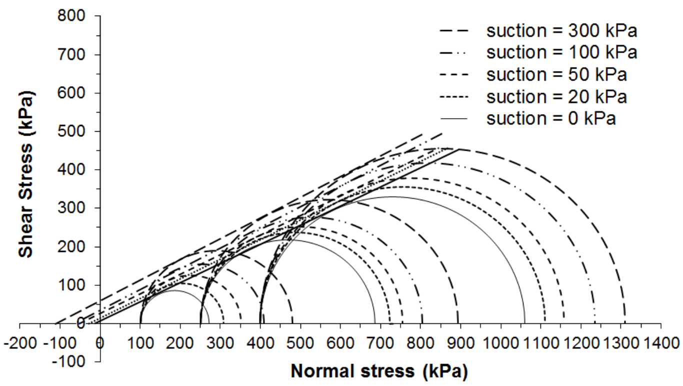

Figure 6. Mohr-Coulomb failure envelopes.

The angle of friction was found to remain very similar for a matric suction range of 0 to 300 kPa (Table 4). The cohesion values remained between 4.8 and 61 kPa for the same range of suction (Table 4). These results show that the cohesion decreased with a decrease in matric suction as the soil underwent the wetting process. Similar findings have been reported by several researchers (Lu & Likos 2004; Murray & Sivakumar; Fredlund et al. 2012).

Table 4. Variation of ϕ' and c with applied suctions.

	Suction (kPa)				
Parameter	0	20	50	100	300
ϕ' (°)	26.7	27.1	27.2	27.9	28.0
c (kPa)	4.8	13.9	25.3	37.8	61.0

Figure 7 shows the impact of suction on the cohesion intercept. It can be seen that cohesion decreased non-linearly (Fredlund et al. 2012) with a decrease in suction during the wetting process. This indicates that the angle ϕ^b increased with a decrease in suction to attain a maximum value at saturation.

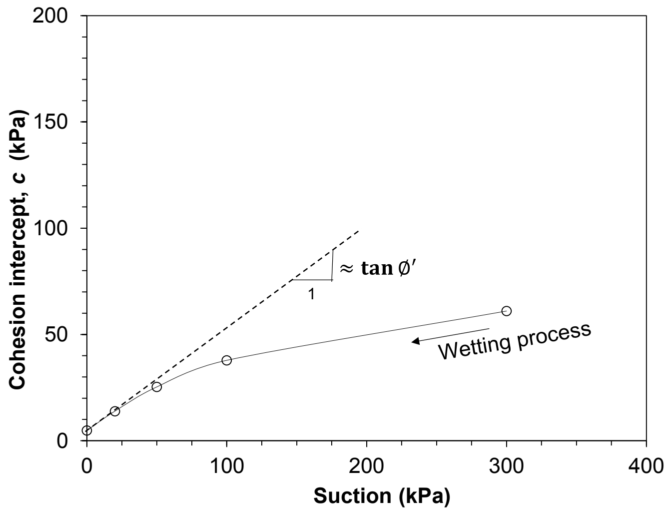

Figure 7. Impact of applied suction on cohesion intercept.

Figure 8 shows the failure envelopes for both saturated and unsaturated conditions of the soil in ($p - u_a$) - q space. The suction stress values corresponding to various applied suctions (i.e., SSCC from shear strength tests) are plotted on the bottom left of Figure 8. The experimental data were best-fitted using Equation (2). The best-fit parameters α and n were found to be 0.018 1/kPa and 1.601, respectively.

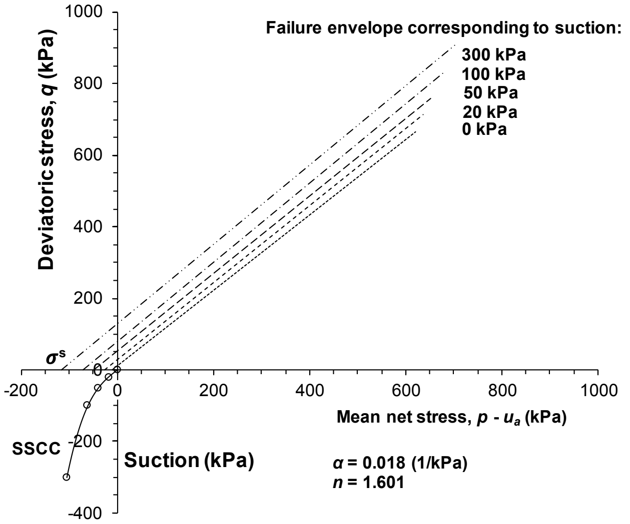

Figure 8. Suction stress characteristic curve from Mohr-Coulomb failure envelopes in (p - u_a) – q space.

Comparing the values of α and n that were obtained from absorption SWCCs (Table 3) and that from SSCC based on the shear strength tests (Fig. 8), it can be noted that the value of α was lower and the value of n was higher in case of the latter. The differences in the best-fit model parameters are attributed to the inclusion of WP4C test results in case of SWCCs in order to cover a large range of suction, whereas the SSCC from the shear strength tests was based on a suction range of 300 to 0 kPa.

4.3 *Comparison of SSCCs based on absorption SWCCs and shear strength tests*

Figure 9 presents the SSCCs that were established based on the absorption SWCCs and the shear strength tests on saturated and unsaturated soil specimens of the soil. The shapes of the SSCCs can be found to be similar from both approaches.

At a suction of 500 kPa, a difference in the suction stress based on the SWCC at confining stress of 400 kPa and the SSCC from the shear strength tests was found to be about 12 kPa. At smaller suctions and at lesser confining stresses, the differences were lesser.

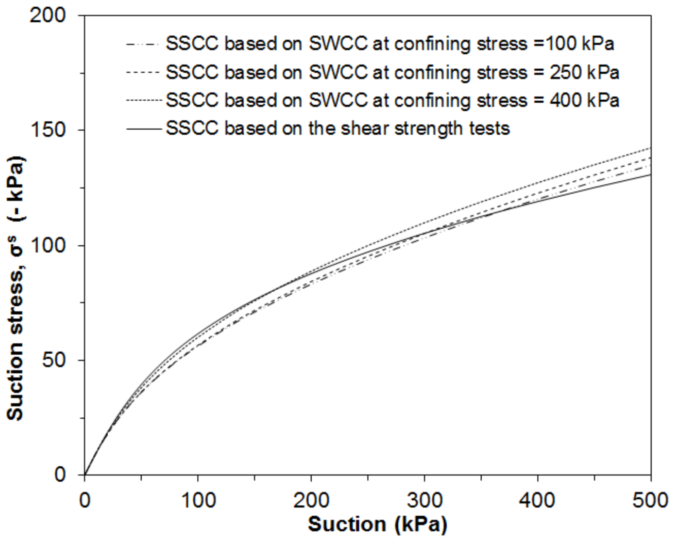

Figure 9. Suction stress characteristic curves (SSCCs) in terms of suction from SWCCs and shear strength tests.

5 CONCLUSIONS

Suction-controlled triaxial shear strength tests were carried out on compacted specimens of a prepared soil that had grain-size fractions similar to that of collapsible soils. The tests were carried out at several confining stresses and matric suctions. The water volume and total volume changes enabled establishing the absorption SWCCs of the soil at predetermined confining stresses. Based on the suction stress approach the suction stress characteristic curves of the soil were established from the absorption SWCCs. The specimens were sheared at several matric suctions. The SSCC of the soil was established from the shear strength test results.

The impact of confining stress on the volumetric strain of the soil was distinct; however, its influence on SWCC and SSCC was found to be insignificant. The SSCCs based on the shear strength tests and SWCCs were found to be very similar with a difference in the magnitude of suction stress of less than about 12 kPa. The findings from study emphasized the strong linkage between SWCC (i.e., the constitutive relation between suction and degree of saturation) and SSCC (i.e., the constitutive relation between suction stress and suction) for collapsible soils that underwent wetting process under high applied stresses.

6 ACKNOWLEDGEMENTS

The first author acknowledges the scholarship provided by the Ministry of Higher Education and Scientific research Iraq, for this research work undertaken at Cardiff University.

7 REFERENCES

Baille, W., Tripathy, S. & Schanz, T. 2014. Effective stress in clays of various mineralogy. *Vadose Zone Journal* 13(5).

Barden, L., McGown, A. & Collins, K. 1973. The collapse mechanism in partly saturated soil. *Engineering Geology* 7(1): 49–60.

Derbyshire, E. and Mellors, T.W. 1988. Geological and geotechnical characteristics of some loess and loessic soils from China and Britain: A comparison. *Engineering Geology* 25(2–4): 135–175.

Fredlund, D.G., Rahardjo, H. & Fredlund, M.D. 2012. *Unsaturated soil mechanics in engineering practice*. Wiley, New York.

Lawton, E.C., Fragaszy, R.J. & Hetherington, M.D. 1992. Review of wetting-induced collapse in compacted soil. *Journal of Geotechnical Engineering* 118(9): 1376–1394.

Leong, E.C., Tripathy, S. & Rahardjo, H. 2003. Total suction measurement of unsaturated soils with a device using the chilled-mirror dew-point technique. *Géotechnique* 53(2): 173–182.

Lu, N., Godt, J.W. & Wu, D.T. 2010. A closed-form equation for effective stress in unsaturated soil. *Water Resources Research* 46(5).

Lu, N. & Likos, W.J. 2004. *Unsaturated soil mechanics*. John Wiley & Sons, New York

Lu, N. & Likos, W.J. 2006. Suction stress characteristic curve for unsaturated soil. *Journal of Geotechnical and Geoenvironmental Engineering* 132(2): 131–142.

Murray, E. & Sivakumar, V. 2010. Unsaturated soils: a fundamental interpretation of soil behaviour. Wiley Blackwell, UK.

Ng, C.W.W. & Menzies, B. 2007. *Advanced unsaturated soil mechanics and engineering*. Taylor & Francis, London.

Oh, S. & Lu, N. 2014. Uniqueness of the suction stress characteristic curve under different confining stress conditions. *Vadose Zone Journal* 13(5).

Oh, S., Lu, N., Kim, T. & Lee, Y.H. 2013. Experimental validation of suction stress characteristic curve from nonfailure triaxial K_0 consolidation tests. *Journal of Geotechnical and Geoenvironmental Engineering* 139(9): 1490–1503.

Oh, S., Lu, N., Kim, Y.K., Lee, S.J. & Lee, S.R. 2012. Relationship between the soil-water characteristic curve and the suction stress characteristic curve: experimental evidence from residual soils. *Journal of Geotechnical and Geoenvironmental Engineering* 138(1): 47–57.

Pereira, J.H. & Fredlund, D.G. 2000. Volume change behaviour of collapsible compacted Gneiss soil. *Journal of Geotechnical and Geoenvironmental Engineering* 126(10): 859–946.

Rampino, C., Mancuso, C. & Vinale, F. 1999. Laboratory testing on an unsaturated soil: equipment, procedures, and first experimental results. *Canadian Geotechnical Journal* 36(1): 1–12.